Structural Studies of Inhibition of *S*-Adenosylmethionine Synthetase by Slow, Tight-Binding Intermediate and Product Analogues[†]

George D. Markham* and Robert S. Reczkowski[§]

Institute for Cancer Research, Fox Chase Cancer Center, 333 Cottman Avenue, Philadelphia, Pennsylvania 19111-2497

Received October 31, 2003

ABSTRACT: *S*-Adenosylmethionine synthetase (ATP: L-methionine *S*-adenosyltransferase) catalyzes a two-step reaction in which tripolyphosphate (PPPi) is a tightly bound intermediate. Diimidotriphosphate (O_3P-NH-PO_2-NH-PO_3; PNPNP), a non-hydrolyzable analogue of PPPi, is the most potent known inhibitor of AdoMet synthetase with a K_i of 2 nM. The structural basis for the slow, tight-binding inhibition by PNPNP has been investigated by spectroscopic methods. UV difference spectra reveal environmental alterations of aromatic protein residues upon PNPNP binding to form the enzyme·$2Mg^{2+}$·PNPNP complex, and more extensive changes upon formation of the enzyme·$2Mg^{2+}$·PNPNP·AdoMet complex. Stopped-flow kinetic studies of complex formation revealed that two slow isomerizations follow PNPNP binding in the presence of AdoMet, in contrast to the lower affinity, rapid-equilibrium binding in the absence of AdoMet. ^{31}P NMR spectra of enzyme complexes with PNPNP revealed electronic perturbations of each phosphorus atom by distinct upfield chemical shifts for each of the three phosphoryl groups in the enzyme·$2Mg^{2+}$· PNPNP complex, and further upfield shifts of at least 2 resonances in the complex with AdoMet. Comparison of the chemical shifts for the enzyme-bound PNPNP with the enzyme complexes containing either the product analogue O_3P-NH-PO_3 or O_3P-O-PO_2-NH-PO_3 indicates that the shifts on binding are largest at the binding sites corresponding to those for the α and γ phosphoryl groups of the nucleotide (-3.1 to -4.1 ppm), while the resonance at the β phosphoryl group position shifts by -2.1 ppm. EPR spectra of Mn^{2+} complexes demonstrate spin coupling between the two Mn^{2+} in both enzyme·$2Mn^{2+}$· PNPNP and enzyme·$2Mn^{2+}$·PNPNP·AdoMet, indicating that the metal ions have comparable distances in both cases. The combined results indicate that formation of the highest affinity complex is associated with protein side chain rearrangements and increased electron density at the ligand phosphorus atoms, likely due to ionization of an -NH- group of the inhibitor. The energetic feasibility of ionization of a -NH- group when two Mg^{2+} ions are bound to O_3P-NH-PO_3 is supported by density functional theoretical calculations on model chelates. This mode of interaction is uniquely available to compounds with P−NH−P linkages and may be possible with other proteins in which multiple cations coordinate a polyphosphate chain.

The only known biosynthetic route to *S*-adenosylmethionine (AdoMet), the predominant alkylating agent in all cells, is the reaction of ATP and L-methionine catalyzed by *S*-adenosylmethionine synthetase (ATP:L-adenosyltransferase) (*1−3*). The multitude of metabolic roles of AdoMet and its involvement in modulation of cell growth has res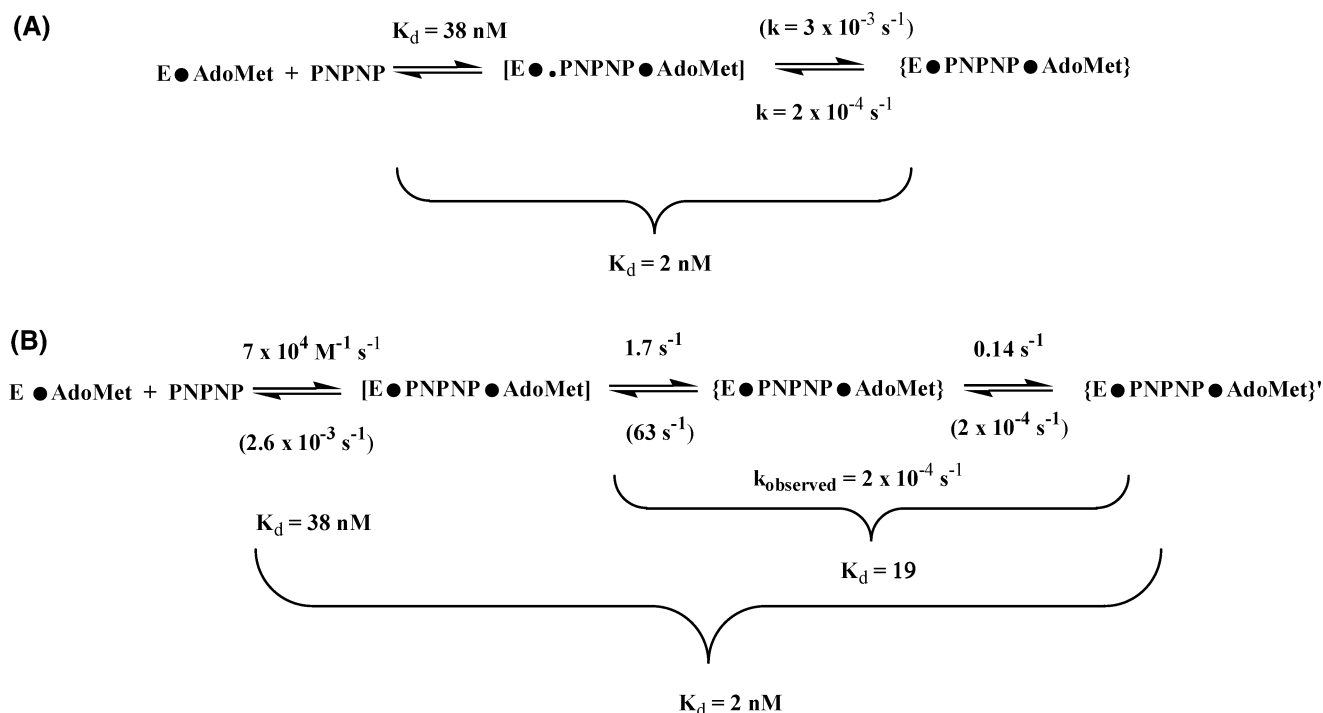ulted in an enduring search for inhibitors with in vivo and in vitro utility (*4−10*). These investigations have included the synthesis of numerous analogues of the methionine substrate (*4−9, 11*). Some of the methionine analogues have had substantial use because of their ability to enter cells, although they have had at best micromolar affinity for AdoMet synthetase (*12−14*). More potent in vitro inhibitors, with K_i values in the low micromolar range, have been prepared as bisubstrate analogues that link portions of methionine to the reactive 5′ position of the nucleotide substrate (*10, 15−19*). We have described mechanism-based inhibition of AdoMet synthetase by diimidotriphosphate (O_3P-NH-PO_2-NH-PO_3; PNPNP),[1] a non-hydrolyzable analogue of the reaction intermediate (*20*). PNPNP was found to be a slow-binding inhibitor of the prototype *Escherichia coli* enzyme with a 2 nM dissociation constant in the presence of AdoMet (Scheme 1A). In the absence of AdoMet, PNPNP was a simple competitive inhibitor with a K_i of 0.5 μM. The

* To whom correspondence should be addressed: Institute for Cancer Research, Fox Chase Cancer Center, 333 Cottman Avenue, Philadelphia, PA 19111-2497. Telephone: 215-728-2439. Fax: 215-728-3574. E-mail GD_Markham@fccc.edu.

§ Present Address: Department of Biochemistry, Temple University School of Medicine, Philadelphia, PA 19140.

[1] Abbreviations: AMPPNP, adenylylimidotriphosphate (β-γ imido-ATP); PNPNP, diimidotriphosphate (O_3P-NH-PO_2-NH-PO_3); PNP, imidodiphosphate (O_3P-NH-PO_3); PPNP, imidotriphosphate (O_3P-O-PO_2-NH-PO_3).

Scheme 1[a]

(A)

$$K_d = 38 \text{ nM} \qquad (k = 3 \times 10^{-3} \text{ s}^{-1})$$

$$E \bullet AdoMet + PNPNP \rightleftharpoons [E \bullet .PNPNP \bullet AdoMet] \rightleftharpoons \{E \bullet PNPNP \bullet AdoMet\}$$

$$k = 2 \times 10^{-4} \text{ s}^{-1}$$

$$K_d = 2 \text{ nM}$$

(B)

$$7 \times 10^4 \text{ M}^{-1} \text{ s}^{-1} \qquad 1.7 \text{ s}^{-1} \qquad 0.14 \text{ s}^{-1}$$

$$E \bullet AdoMet + PNPNP \rightleftharpoons [E \bullet PNPNP \bullet AdoMet] \rightleftharpoons \{E \bullet PNPNP \bullet AdoMet\} \rightleftharpoons \{E \bullet PNPNP \bullet AdoMet\}'$$

$$(2.6 \times 10^{-3} \text{ s}^{-1}) \qquad (63 \text{ s}^{-1}) \qquad (2 \times 10^{-4} \text{ s}^{-1})$$

$$k_{observed} = 2 \times 10^{-4} \text{ s}^{-1}$$

$$K_d = 38 \text{ nM}$$

$$K_d = 19$$

$$K_d = 2 \text{ nM}$$

[a] (A) Original scheme; (B) expanded scheme. Calculated values are in parentheses.

enhanced affinity of PNPNP in the presence of AdoMet reprises the AdoMet activation of the rate of PPPi hydrolysis. In conjunction with the finding that an Arg244Leu mutation at the PPPi binding site led to both a 1000-fold reduced hydrolytic activity and a 5000-fold decrease in affinity for PNPNP, it appears that PNPNP has properties similar to a transition state analogue (*20, 21*). Our studies also showed that imidodiphosphate (O_3P-NH-PO_3, PNP), a non-hydrolyzable analogue of the pyrophosphate product, was a slow binding inhibitor in the presence of AdoMet, with 400-fold lower affinity than PNPNP. The distinguishing feature of these compounds is the presence of a potentially ionizable -NH- group(s) at the position corresponding to the bridge oxygen(s) of the natural intermediate and product. In light of AdoMet synthetase crystal structures which showed that two divalent cation activators (Mg^{2+} or Mn^{2+}) are ligated to the polyphosphate chain in complexes with PPi plus Pi, or ADP plus Pi (*22*), it was proposed that deprotonation of one or both of the bridging -NH- groups might be related to the high affinity and slow binding rates (Figure 1, structure A → B or C) (*20*).

In the present work, we have used a variety of spectroscopic methods to investigate the interactions of PNPNP and PNP with AdoMet synthetase, and the effects of AdoMet on the enzyme complexes. Diimidotriphosphate has been synthesized with ^{15}N enrichment for NMR studies. The energetic relationships of various models of the enzyme complexes have been investigated by density functional theoretical calculations. The studies reveal perturbations of both protein conformation and the electronic environment of the phosphorus atoms upon complex formation, and suggest a structural basis for the slow binding and high affinity.
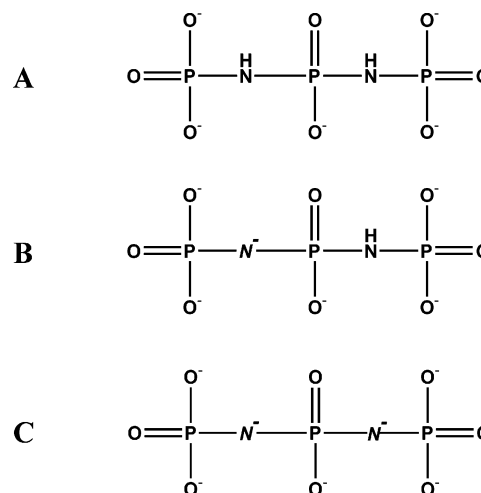
FIGURE 1: (A−C) Possible protonation states for diimidotriphosphate bound to AdoMet synthetase.

EXPERIMENTAL PROCEDURES

Most reagents were purchased from Sigma. AdoMet was purchased from Research Biochemicals International. L-[Methyl-^{14}C]methionine was bought from Dupont-NEN. Ecoscint scintillation fluid was purchased from National Diagnostics. The purification and characterization of *E. coli* AdoMet synthetase have been previously described (*21*). Enzyme concentrations were determined from the absorbance at 280 nm using an extinction coefficient of 1.3 (mg/mL-cm)$^{-1}$ and a molecular weight of 43 000 for each subunit of the tetramer. AdoMet synthetase activity was determined from [^{14}C]-AdoMet formation using a filter binding method (*23*). Assays were performed in the presence of 10 mM ATP and 0.5 mM L-[^{14}C-methyl]-methionine in 50 mM Hepes·$(CH_3)_4N^+$ at pH 8.0 with 50 mM KCl, and 20 mM $MgCl_2$. Before use, enzyme was exchanged into 50 mM Hepes·K^+, 50 mM KCl,

10% glycerol, 1 mM dithiothreitol, pH 8.0, by gel filtration. $Na_5 \cdot PNPNP$ was synthesized as reported (*20*, *24*). [Mono-^{15}N]-PNPNP was prepared in the Organic Synthesis Facility at the Fox Chase Cancer Center by the same route, using $(^{15}NH_4)2SO_4$ as the source of nitrogen in the first step of the synthesis. ^{31}P NMR spectra of a 10 mM solution of [^{15}N]-PNPNP at pH 8.0 showed chemical shifts of -1.6 ppm (middle P) and 0.10 ppm (end P) with $^1J(P-N) = 21$ and $^2J(P-P) = 4$ Hz. Titration of 10 mM PNPNP with $MgCl_2$ at pH 8.0 showed changes in chemical shifts that maximized at 1:1 molar ratio of $Mg^{2+} \cdot PNPNP$; in the 1:1 complex the relative ^{31}P chemical shifts of the end and middle P are inverted. The chemical shifts of $Mg^{2+} \cdot PNPNP$ complex are 2.6 ppm (middle P) and 1.2 ppm (end P), and the coupling constants are $^2J(P-P) = 6$ Hz and the $^1J(P-N)$ of 21 Hz. ^{15}N NMR spectra of [mono-^{15}N]PNPNP showed a chemical shift of 58 ppm from NH_4^+ and a change to 59 ppm in the presence of one equivalent of $MgCl_2$. In all experiments, samples were buffered with 50 mM Hepes·K^+, 50 mM KCl, 10% glycerol, 1 mM dithiothreitol, pH 8.0.

UV Spectral Studies. UV difference spectra were obtained on a Hewlett-Packard HP8453 spectrophotometer (1-nm resolution). Spectra were accumulated for 25 s to reduce noise. Spectra were separately obtained for the enzyme and ligand(s), and then the solutions were mixed to allow complex formation. Spectra obtained before and after mixing were digitally subtracted to yield the difference spectrum.

Stopped-flow experiments employed a pneumatically driven Hi-Tech SFA-20 accessory in a HP8452 spectrophotometer (2-nm resolution). Data acquisition was triggered by a microswitch activated by the stopping syringe. Spectra (240−300 nm) were acquired every 0.1 s, which is the fastest possible with this spectrophotometer. The dead time of this configuration is 125 ms (*25*). Single wavelength time course data were fit to a double exponential model using the program Scientist (MicroMath Inc.). Subsequently time-dependent spectral data were analyzed using a global multiwavelength analysis method implemented in the Pro-K·2000 software (Applied Photophysics Ltd.). The rate constants obtained by the two analysis protocols were indistinguishable.

NMR Methods. NMR spectra were recorded on Bruker Avance DMX 600 and DRX 300 spectrometers. ^{31}P spectra were obtained at 121.4 MHz and ^{15}N spectra at 60.1 MHz. Samples included either 5% D_2O for locking, or in some cases 99% D2O. Data were processed using either the program Felix 2000 (MSI Inc.) or the program Spinworks v. 1.2 (*26*). Chemical shifts are referenced to external 85% H_3PO_4 or 0.1 M $(^{15}NH_4)_2SO_4$, as appropriate. The temperature was maintained at 25 °C unless noted.

^{15}N spectra were obtained using a 30° pulse every 3 s; the chemical shift range from -100 to $+100$ ppm was digitized at 0.7 Hz/point. The negative magnetogyric ratio of ^{15}N can result in a negative nuclear Overhauser effect (NOE) upon ^1H decoupling, with attendant loss of signal intensity, in complexes with long rotational correlation times. Therefore, spectra in H_2O were obtained without decoupling, with ^1H decoupling, and with inverse-gated ^1H decoupling to remove proton splittings while avoiding possible signal reduction from a negative NOE. ^{15}N spectra of samples in D_2O were obtained without decoupling. In ^{31}P studies, a 60° pulse was applied every 2 s and the spectral width covered
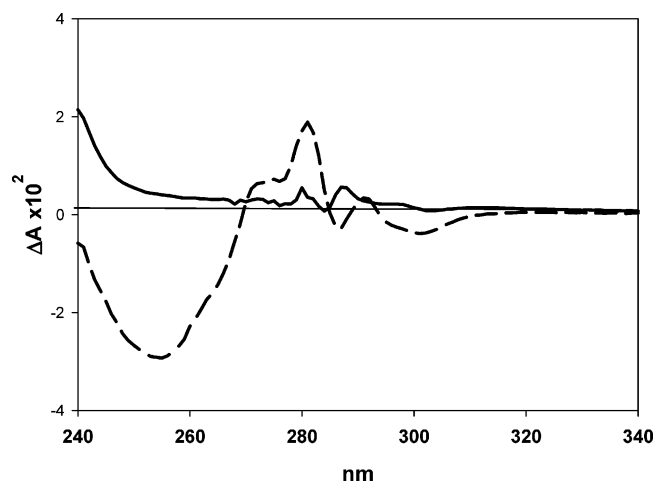

FIGURE 2: UV difference spectra for formation of PNPNP complexes from enzyme and ligands. The solid line is the difference spectrum for formation of the enzyme·$2Mg^{2+}$·PNPNP complex, and the dotted line is the difference spectrum for formation of the enzyme·$2Mg^{2+}$·AdoMet·PNPNP complex. In both cases, the reference samples contained separate samples of enzyme and all ligands except PNPNP. Solutions contained (final concentrations) 23 μM enzyme subunits, 42 μM PNPNP, and 1.4 mM $MgCl_2$ in 50 mM Hepes/KOH, 50 mM KCl, 10% glycerol, 1 mM DTT, pH 8.0. Where present, the AdoMet concentration was 42 μM.

-25 to 25 ppm, at a resolution of 0.7 Hz/point; ^1H decoupling was not used.

At least 32 000 transients were averaged for ^{15}N spectra; 4000 transients were collected for each ^{31}P spectrum, except in the case of the unstable enzyme·$2Mg^{2+}$·PNPNP·AdoMet complex for which 500 transients were collected at 4 °C.

EPR Methods. EPR spectra were obtained at 4 °C on a computer interfaced Varian E-109 spectrometer operating at 9.1 G Hz. Spectra were recorded with 10 G modulation amplitude, 100 mW microwave power, with a sweep rate of 4 G/s and were digitized at 0.25 G/point. Samples for EPR spectra were prepared in the same fashion as those for NMR except that $MnCl_2$ replaced $MgCl_2$. In all samples Mn^{2+} was present at less than the binding stoichiometry of 2 equiv per active site.

Computational Methods. Free energies for $(Mg^{2+} \cdot O_3P-NH-PO_3)^{2-}$ and $((Mg^{2+})_2 \cdot O_3P-NH-PO_3)^0$, as well as the reference compounds $H_4 \cdot O_3P-NH-PO_3$ and H_2O, were evaluated using the hybrid density functional B3LYP method in conjunction with the 6-311++G** basis set (*27*, *28*), as implemented in *Gaussian-98* (*29*). Optimized geometries, frequency analyses, thermal and entropic corrections to 298 K were computed. Frequency analyses indicated that stable states were characterized in each case. These calculations are implicitly in vacuo. NMR chemical shift anisotropies were calculated using the gauge independent atomic orbital (GIAO) method as implemented in *Gaussian-98* (*30*). The GIAO method has been shown to provide good estimates for chemical shielding tensors (*31*, *32*).

RESULTS

UV Spectroscopy. The possibility of protein conformational alterations upon formation of complexes with PNPNP and PNP was investigated using UV difference spectroscopy (Figure 2). The spectra shown in Figure 2 indicate perturbations of several chromophores upon formation of the enzyme·
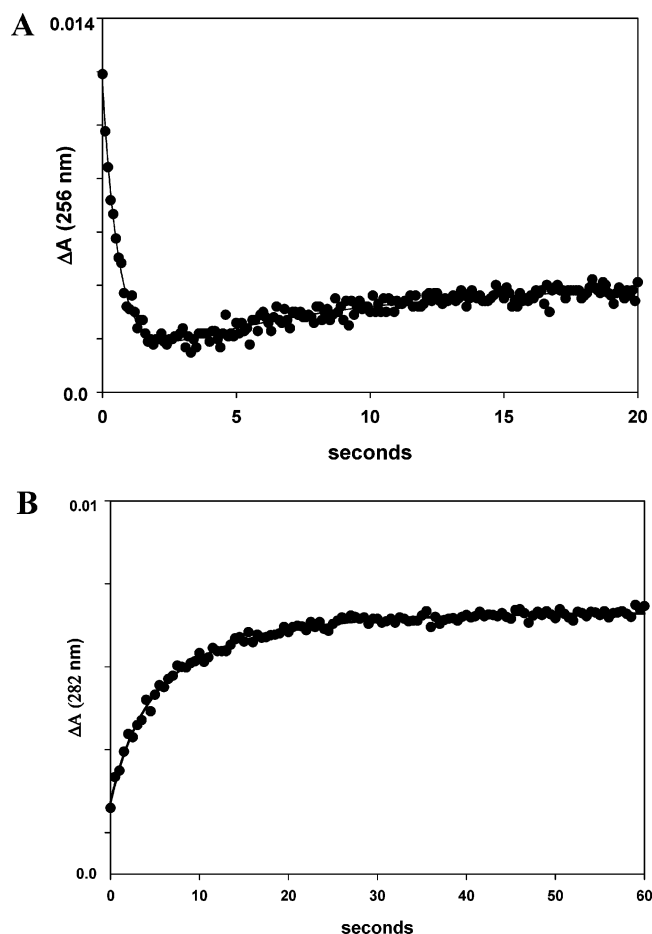
A

B

FIGURE 3: Stopped-flow time courses of UV changes upon formation of the enzyme·$2Mg^{2+}$·AdoMet·PNPNP complex from free enzyme and ligands. Panel A illustrates the time course monitored at 256 nm and panel B is the change monitored at 282 nm. Note the longer time scale in panel B, which emphasizes the slower kinetic phase. Data points are shown as (●), and the lines are the curve fits for a double exponential with rate constants of 1.7 and 0.14 s^{-1}. Solutions contained (final concentrations): 21 μM enzyme subunits, 125 μM PNPNP, 55 μM AdoMet, and 6 mM $MgCl_2$ in 50 mM Hepes/KOH, 50 mM KCl, pH 8.0; T = 25 °C.

$2Mg^{2+}$·AdoMet·PNPNP complex (the reference spectrum had all components except PNPNP). Omission of AdoMet resulted in distinct and less intense difference spectra. When PPPi, PPi, or the product analogue PNP replaced PNPNP the difference spectra were similar to those with PNPNP, both in the presence and absence of AdoMet (not shown).

Stopped-Flow Kinetics. The UV difference spectrum that accompanies formation of the enzyme·$2Mg^{2+}$·AdoMet· PNPNP complex allowed measurement of the rates of the slow process(es) associated with the inhibition. Previous experiments which monitored the onset of inhibition at low enzyme concentration showed the presence of an isomerization step(s) following binding resulting in an overall equilibrium constant of 2 nM, and a net dissociation rate of 0.0002 s^{-1} (Scheme 1A) (20).

Stopped-flow measurements were carried out by mixing enzyme with a solution of AdoMet, Mg^{2+}, and PNPNP; the UV absorption change throughout the 300−240 nm spectral region was monitored, and revealed a distinctly biphasic time dependence to the changes. Figure 3A shows the time course observed at 256 nm; the time dependence reflects two processes with rates of 1.7 and 0.14 s^{-1}. The same rates were

Table 1: ^{31}P NMR Chemical Shifts^a

	ends	middle
PNPNP	+0.1	−1.6
Mg^{2+}·PNPNP	+1.2	+2.6
Mg^{2+}·PNP	+3.3	
PNP	+2.2	

	γ	β	α
Mg^{2+}·AMPPNP	+0.2	−4.5	−8.7

	enzyme-bound		
E·$2Mg^{2+}$·PNPNP	+1.4	−0.8	−3.2
E·$2Mg^{2+}$·PNPNP·AdoMet	+0.5	−1.9	−2.9
E·$2Mg^{2+}$·PNP·AdoMet	+4.1	−2.2	
E·$2Mg^{2+}$·PPNP·AdoMet	−3.3	−8.2	−11.1

^{a} Chemical shifts are in ppm from 85% H_3PO_4. Spectra were obtained at 25 °C except for the E·$2Mg^{2+}$·PPNP·AdoMet complex, which for the spectrum was obtained at 4 °C. Solutions contained 50 mM Hepes/ KOH, 50 mM KCl, 10% glycerol, 1 mM DTT, pH 8.0. Other conditions are listed in the legend to Figure 4.

seen at 282 nm as illustrated in a longer time course in Figure 3B. When the concentrations of the ligands were all doubled the rates did not change, indicating that unimolecular events after the initial binding step were being monitored. Furthermore, the same rates were observed when PNPNP was added to a mixture of enzyme, AdoMet, and Mg^{2+}. The absence of a concentration dependence for the observed rates at 10^{-4} M reactant concentrations shows that the bimolecular rates of binding are $>10^4$ M^{-1} s^{-1}. Observation of PNPNP binding by protein fluorescence changes on the <100 ms time scale revealed a rate that was dependent on PNPNP concentration with a second-order rate constant of 7×10^4 M^{-1} s^{-1}, comparable to the rate of PPPi binding (33). Thus, the UV absorption changes unmask a second isomerization of the enzyme·AdoMet·$2Mg^{2+}$·PNPNP complex that was not previously apparent (Scheme 1B).

When PNP replaced PNPNP, all spectral changes were complete within the dead time of the experiment (0.12 s) consistent with lower affinity of PNP and the ~25-fold more rapid onset of inhibition observed in steady-state kinetic experiments (K_i = 0.8 μM, with a net dissociation rate of 0.005 s^{-1}). The UV changes for both PNPNP and PNP binding in the absence of AdoMet were completed within the dead time of the experiment, consistent with the rapid equilibrium demands of the competitive inhibition kinetics (20). All spectral changes were completed within the experimental dead time when PPPi was the ligand.

NMR STUDIES

^{31}P NMR. ^{31}P NMR spectra were obtained for PNPNP in solution and bound to AdoMet synthetase as a probe of the environment of the phosphoryl groups of PNPNP when bound to the enzyme, and the influence of AdoMet. The chemical shifts for the various species are collected in Table 1.

Mg^{2+} binding to PNPNP at pH 8.0 resulted in a larger change in the ^{31}P chemical shifts for the central P (from −1.6 to +2.6 ppm) than for the terminal P (+0.1 to + 1.2 ppm). The pK for ionization of 10 mM Mg^{2+}·PNPNP was obtained by monitoring the chemical shift changes between pH 3 and 9; the chemical shifts become more positive at higher pH, by 1 ppm for the terminal phosphorus atoms and 4.5 ppm
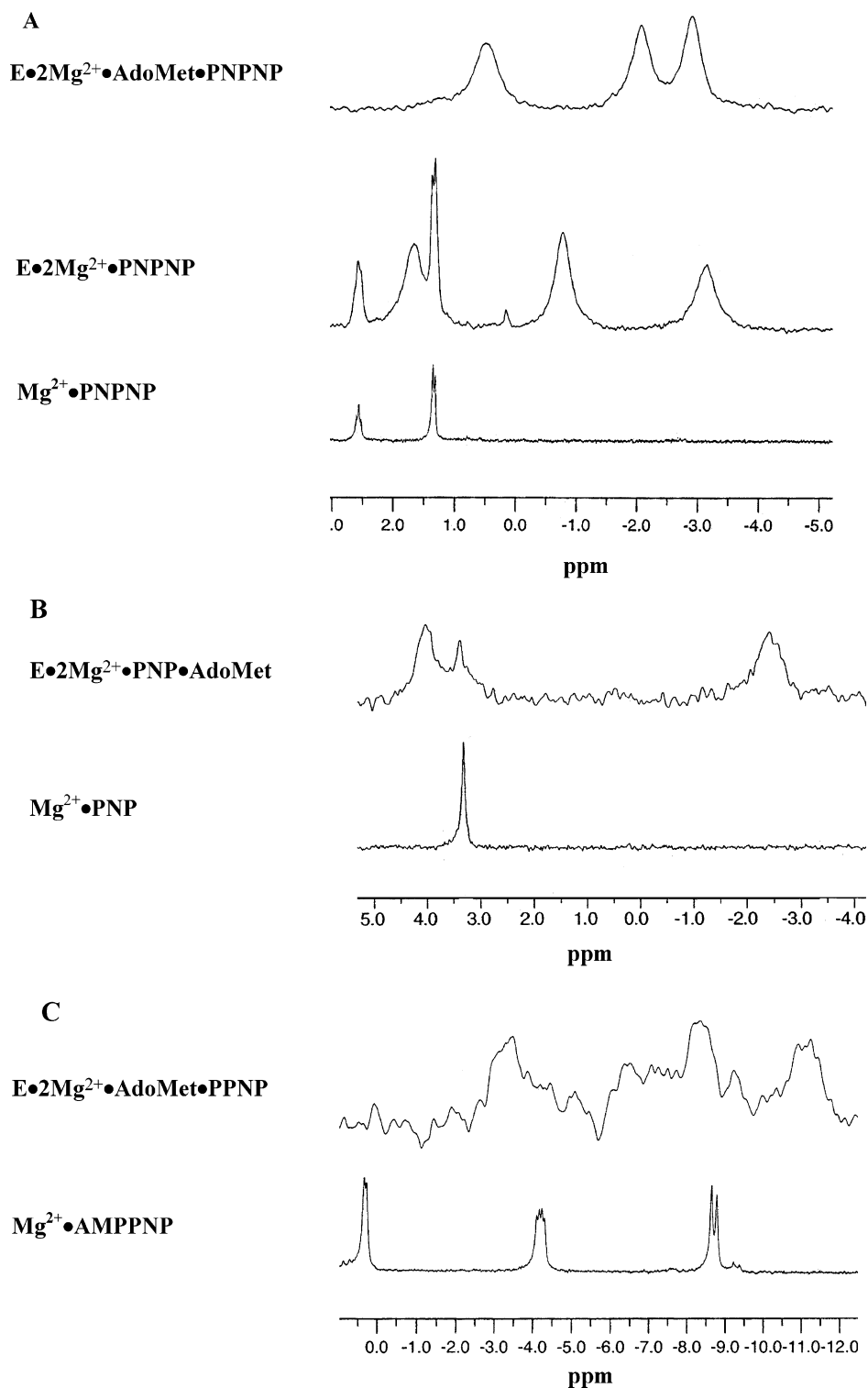
FIGURE 4: ^{31}P NMR spectra of imidophosphates in solution and bound to AdoMet synthetase. (A) Samples contained 1 mM PNPNP, and 2 mM MgCl$_2$ in 50 mM Hepes/KOH, 50 mM KCl, 10% glycerol, 1 mM DTT, pH 8.0. Where present, the AdoMet concentration was 2.3 mM and the enzyme concentration was 1 mM. The small signal at 0.3 ppm in the E·2Mg^{2+}·PNPNP complex stems from an unknown degradation product. (B) The samples were as in panel A but contained 1 mM PNP in place of PNPNP. (C) The sample for the top spectrum contained 1 mM enzyme (active sties), 1 mM AMPPNP, 5 mM methionine, and 2 mM MgCl$_2$, and in the sample for the lower spectrum the protein was omitted. Exponential line broadening functions of 2 Hz were used in samples without protein, 6 Hz for enzyme complexes in panels A and B and 20 Hz for panel C. Data were obtained at 25 °C in panels A and B, and at 4 °C for panel C.

for central phosphorus, consistent with the larger pH sensitivity of the β-phosphorus of AMPPNP (*34*). The data indicate a pK value of 6.0; an analogous experiment with Mg^{2+}·PPPi showed a pK of 4.7. The ionizations reflect formation of the trianionic complex at elevated pH (*35*).

^{31}P of Enzyme Complexes. ^{31}P NMR has provided valuable insights into the active sites of many proteins that bind phosphorus containing ligands (*36−38*). The ^{31}P signals for the enzyme·2Mg^{2+}·AdoMet·PNPNP complex occur at +0.5, −1.9, −2.9 ppm, with line widths of 40−45 Hz (Figure 4A).

Thus, the symmetry of PNPNP is lost upon binding to the protein. The observation of three distinct resonances shows that bound PNPNP does not readily reorient end-to-end, consistent with the oriented cleavage of the enzyme-bound PPPi that is formed as a reaction intermediate (*23*). Spectra obtained after addition of a slight molar excess of PNPNP over enzyme active sites showed sharp peaks with chemical shifts corresponding to those observed for $Mg^{2+} \cdot$PNPNP in the absence of protein, demonstrating slow exchange between free and bound species; the line widths of the free PNPNP were <5 Hz, providing an upper limit on the exchange rate with the enzyme-bound complex.

In the enzyme$\cdot 2Mg^{2+} \cdot$PNPNP complex, peaks were observed at $+1.4$, -0.8, and -3.2 ppm (Figure 4A), with line widths of 40–45 Hz, reinforcing the asymmetric environment of enzyme-bound PNPNP. Thus, the chemical shifts for at least two of the ^{31}P differ when AdoMet is bound. Excess PNPNP was again in slow exchange on the NMR time scale (Figure 4A). Although PNPNP is a competitive inhibitor of PPPi hydrolysis in the absence of AdoMet, the slow catalytic rate of 0.08 s^{-1} is compatible with both slow exchange on the NMR time scale and the reversibility of inhibitor binding.

Spectra of a complex with the product analogue PNP were obtained to aid in resonance assignments. PNP occupies the binding sites for the product PPi which correspond to those of the α and β phosphoryl groups of the nucleotide triphosphate substrate. Spectra of the enzyme-bound PNP were only obtained in the presence of AdoMet due to the relatively weak binding in the absence of AdoMet. Signals were observed for enzyme$\cdot 2Mg^{2+} \cdot$AdoMet$\cdot$PNP with chemical shifts of $+4.5$ and -1.9 ppm, compared to $+3.3$ ppm for $Mg^{2+} \cdot$PNP and $+2.2$ ppm for unchelated PNP (Figure 4B). The symmetry of PNP is also lost upon binding to the protein. Not surprisingly given its 0.5 μM dissociation constant, bound PNP is in slow exchange with the free species, as shown by the signal from $Mg^{2+} \cdot$PNP in Figure 4B.

The ^{31}P spectrum of the enzyme$\cdot 2Mg^{2+} \cdot$AdoMet$\cdot$PPNP complex, formed by the reaction of methionine with AMP-PNP, showed three signals at -3.3, -8.2, and -11.1 ppm, compared to $+0.2$ (Pγ), -4.5 (Pβ), and -8.7 (Pα) ppm in unbound $Mg^{2+} \cdot$AMPPNP (Figure 4C). Although the data were obtained at 4°, the complex decomposed due to slow reorientation of PPNP and hydrolysis of the P–O–P linkage to yield Pi plus PNP (*23*); the instability limited data acquisition time and resulted in the low signal-to-noise ratio. The line widths of the bound PPNP were ~100 Hz, 2–5-fold larger those of the other complexes, at least in part due to the longer rotational correlation time at the reduced temperature. In the absence of methionine, the chemical shifts and line widths of $Mg^{2+} \cdot$AMPPNP were unperturbed from a sample that lacked protein. The dissociation constant of 2 mM for $Mg^{2+} \cdot$AMPPNP binding in the absence of methionine precludes observation of the enzyme$\cdot 2Mg^{2+} \cdot$AMPPNP complex since the majority of the nucleotide could not be bound at achievable protein concentrations (*39*). Assignments of the ^{31}P resonances are proposed below.

^{15}N NMR. We speculated that ^{15}N NMR could provide a definitive determination of whether the nitrogens of enzyme-bound PNPNP were protonated. Reynolds et al. reported a ^{1}J(N–H) of 71 Hz for the imido nitrogen of AMPPNP and PNP, and their Mg^{2+} complexes (*35*). In light of previous

results for ^{15}N-enriched ligands bound to the 280 kDa porphobilinogen synthase, it appeared likely that the nitrogen protonation states in a complex with the 172 kDa AdoMet synthetase could be deduced from comparison of line widths in H_2O and D_2O solutions (*40*). The line widths of a -NH-moiety would be substantially reduced upon conversion to -ND- due to the lesser dipolar broadening by the smaller magnetic moment of the deuteron and the reduction of scalar coupling, and further reduced in an -N^{-}- moiety (*41*). Thus, we synthesized [^{15}N]PNPNP enriched to 95% at one nitrogen in this symmetrical compound.

A ^{15}N chemical shift of 58 ppm was observed for 10 mM PNPNP at pH 8.0 (not shown). The shift changed to 59 ppm in the presence of 1 equiv of Mg^{2+}. The ^{1}J(P–N) was 21 Hz in both cases. Reynolds et al. reported chemical shifts of 56 ppm for both AMPPNP and PNP (*35*), and that the addition of 1 equiv of Mg^{2+} to AMPPNP resulted in a 1 ppm more positive shift. The reported ^{1}J(P–N) coupling constants are similar for both PNP and AMPPNP (27 Hz at pH 11, with nonequivalent couplings of 22 and 32 Hz in AMPPNP at pH 7.2 (*35*)).

In the absence of ^{1}H decoupling the ^{15}N NMR spectrum of PNPNP at pH 8.0 showed that the triplet due to the ^{1}J(P–N) was broadened into a single line with an apparent line width of 80 Hz. The lack of resolved ^{1}H-^{15}N coupling implies that the imido protons exchange rapidly with solvent; in the slow exchange limit the broadening would provide an upper limit on ^{1}J(H–N) of ~10 Hz. Attempts to obtain polarization transfer from ^{1}H to ^{15}N in PNPNP, using the DEPT sequence tuned to J values of 10 or 70 Hz, were unsuccessful. ^{1}H NMR spectra of [^{15}N]PNPNP in H_2O did not reveal the chemical shift of the -NH- proton, supporting ready exchange with bulk solvent. The reported ^{1}H chemical shift for the -NH- proton of AMPPNP is 4.4 ppm at pH 11, showing both that the imido nitrogen is protonated and that the imido hydrogen is in slow exchange with bulk water (*35*). The tetraethyl ester of PNP has pK of 3.8 for deprotonation of the -NH- moiety; the ^{15}N chemical shift change of $+2.5$ ppm upon deprotonation was proposed as representative for this type of nitrogen (*35*).

Unfortunately, no ^{15}N NMR signal was observed for the enzyme$\cdot 2Mg^{2+} \cdot$PNPNP complex in the presence or absence of AdoMet, even after 48 h of data acquisition at 60 MHz. The same samples gave excellent ^{31}P spectra at 121 MHz in less than 1 h, and samples lacking protein yielded ^{15}N spectra in a few minutes. Data were collected for enzyme-bound [^{15}N]PNPNP in D_2O, and in H_2O with and without ^{1}H decoupling, and with inverse gated decoupling (to avoid a potentially signal-reducing negative nuclear Overhauser effect), all to no avail.

To assess potential reasons for the signal absence, various line width contributions for bound PNPNP were estimated as described previously (*40*). At a magnetic field of 14 T, the dipolar contribution to the ^{15}N line width from two directly bonded P is estimated to be 2 Hz (with the estimated protein rotational correlation time of 80 ns (*39*)). A ^{2}H directly attached to the ^{15}N is expected to contribute 10 Hz, whereas a similarly bonded ^{1}H is expected to contribute 50 Hz. Excessive NMR line widths of the enzyme complex cannot thus be attributed to dipolar relaxation from directly attached nuclei. Evaluation of the possible line width contributions from modulation of chemical shift anisotropy
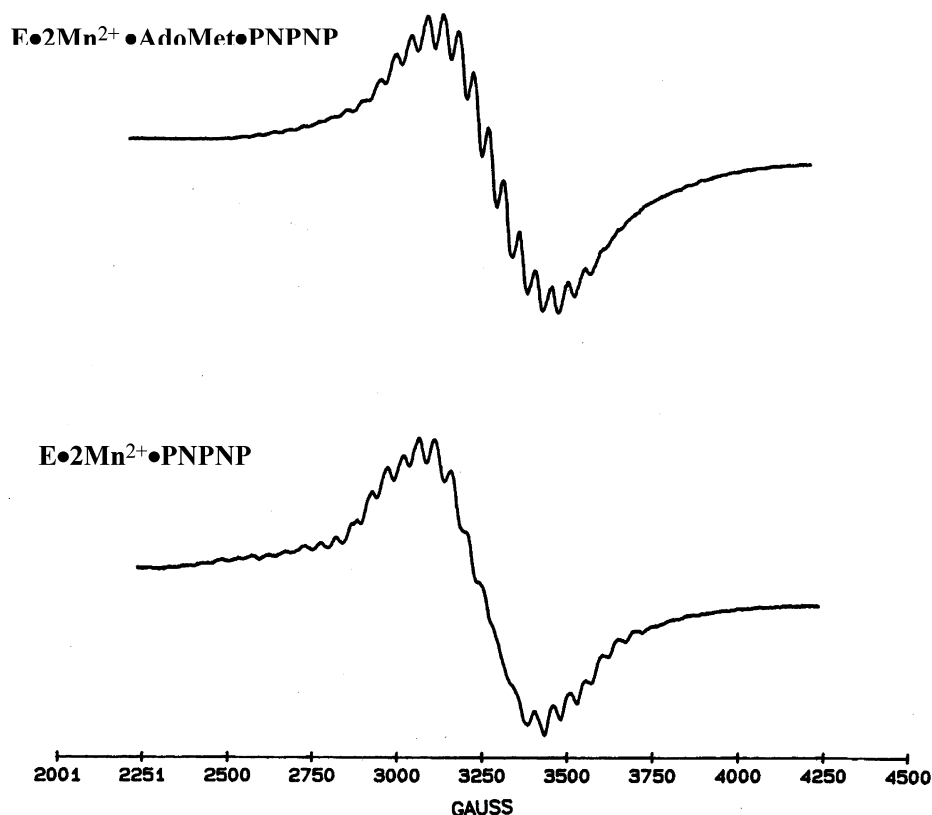
FIGURE 5: EPR spectra of Mn^{2+} complexes with PNPNP bound to AdoMet synthetase. Samples contained 1 mM enzyme (active sties), 1.0 mM PNPNP, and 0.7 mM $MnCl_2$ in 50 mM Hepes/KOH, 50 mM KCl, 10% glycerol, 1 mM DTT, pH 8.0. Where present, the AdoMet concentration was 2.0 mM. Spectra were the average of four scans and were recorded at 4 °C.

(CSA) was complicated by the lack of experimental data for appropriate model compounds. Thus, the ^{15}N CSA was calculated using the gauge independent atomic orbital method (*30*) at the B3LYP/6-311++G** level using optimized geometries of O_3P-NH-PO_3, O_3P-N^--PO_3 and their mono- and di-magnesium complexes. The anisotropy for the -NH- moiety was 130 ±10 ppm in each case while that for the $-N^-$ was 55 ± 15 ppm; these values would contribute ∼40 and ∼8 Hz to the ^{15}N line width of the protein complex at 14 T, respectively. The net line widths for each component of the triplet are estimated to be ∼90 Hz for a -NH- group, ∼50 Hz for a N−D group and ∼10 Hz for an $-N^-$. Thus, the inability to observe a signal for the a bound -NH- group might be attributed to large line widths, but other effects such as chemical exchange phenomena, must contribute to the lack of detectable signals in D_2O, whether -ND- or $-N^-$- groups are present. The formal possibility exists that exceedingly long T_1 relaxation times, ≫10 s, could have led to signal saturation; a relaxation time of this length would make spectral acquisition impractical.

EPR of Mn^{2+} Complexes. To assess whether changes in metal ion ligation might occur upon AdoMet binding to PNPNP, EPR spectra were obtained for the corresponding Mn^{2+} complexes (Figure 5). Previous studies have shown that Mn^{2+} activates as well as Mg^{2+} and is a good probe of metal ion coordination, revealing the proximity of the two divalent cations at the active site (*42*). The spectrum of the E·$2Mn^{2+}$·PNPNP complex displays a large number of lines spaced at 45 G intervals and centered at $g = 2.0$, indicating the presence of a spin-exchange coupled binuclear Mn^{2+} site (*43*). This spectrum was similar to that obtained when

AMPPNP and methionine were allowed to react to form the E·$2Mn^{2+}$·AdoMet·PPNP complex (*42*). The spin-coupled spectrum was observed even when a sub-stoichiometric amount of Mn^{2+} (0.7 equiv per subunit; 0.35 equiv per divalent cation binding site) was present in a sample that had equal concentrations of enzyme active sites, AdoMet and PNPNP. Further addition of Mn^{2+} to 1.8 equiv per subunit did not alter the spectral features, but merely increased the signal intensity. Thus, the two metal ions bind in a cooperative fashion, as seen with the complex formed from AMPPNP plus methionine. When AdoMet was present, the spectral line widths decreased, but the basic features were unaltered (Figure 5). The E·$2Mn^{2+}$·PNPNP complex is the first complex of AdoMet synthetase in which spin coupling of the two metals has been observed when the AdoMet binding site is not occupied, and demonstrates that AdoMet is not required for cluster formation (*42*). When PNP replaced PNPNP a broad envelope centered at $g = 2.0$ was observed; the overall line shape was similar to the spectra in Figure 5, but the hyperfine structure was not resolved, reminiscent of previously reported spectra of PPi complexes (*42*).

Energetic Feasibility of Deprotonation. To evaluate the possibility of deprotonation of a -NH- group at the active site, the free energies for deprotonation of several species were calculated using density functional theory at the B3LYP/6-311++G** level. The calculations were limited to imidodiphosphate for computational expediency. The computed free energies for H^+ dissociation (XH → X^- + H^+) and for the transfer of H^+ to OH^- (XH + OH^- → X^- + H_2O) are compared in Table 2. The transfer of a H^+ to hydroxide (or a similarly basic acceptor) is energetically

Table 2: Deprotonation Free Energies (ΔG_{298}^0) and Free Energies of Proton Transfer to Hydroxide ($\Delta\Delta G_{298}^0$) for Imidodiphosphate Complexes[a]

reaction	ΔG_{298}^0 (kcal/mol)	$\Delta\Delta G_{298}^0$ (kcal/mol)
$H_2O \rightarrow H^+ + OH^-$	389	0
$2H_2O \rightarrow H_3O^+ + OH^-$	225	−174
$H_2O_3P\text{-}NH\text{-}PO_3H_2 \rightarrow$ $H_2O_3P\text{-}N\text{-}PO_3H_2 + H^+$	313	−76
$(Mg^{2+}\cdot O_3P\text{-}NH\text{-}PO_3)^{2-} \rightarrow$ $(Mg^{2+}\cdot O_3P\text{-}N^-\text{-}PO_3)^{3-} + H^+$	523	134
$((Mg^{2+})_2\cdot O_3P\text{-}NH\text{-}PO_3) \rightarrow$ $((Mg^{2+})_2\cdot O_3P\text{-}N\text{-}PO_3)^- + H^+$	333	−56

[a] Free energies at 298 K, in a.u.: H_2O: −76.454890; OH^-: −75.835169; H_3O^+: −76.716093; $H_2O_3P\text{-}NH\text{-}PO_3H_2$: −1192.164620; $(H_2O_3P\text{-}N^-\text{-}PO_3H)^-$: −1191.6165246; $(Mg^{2+}\cdot O_3P\text{-}NH\text{-}PO_3)^{2-}$: −1389.993984; $(Mg^{2+}\cdot O_3P\text{-}N^-\text{-}PO_3)^{3-}$: −1389.159803; $((Mg^{2+})_2\cdot O_3P\text{-}NH\text{-}PO_3)$: −1590.153124; $((Mg^{2+})_2\cdot O_3P\text{-}N^-\text{-}PO_3))^-$: 1589.622463.

favorable for the $(2Mg^{2+}\cdot O_3P\text{-}NH\text{-}PO_3)^0$ complex, but not for $(Mg^{2+}\cdot O_3P\text{-}NH\text{-}PO_3)^{2-}$, in accord with solution experimental data that indicate a pK > 11 for $(Mg^{2+}\cdot O_3P\cdot NH\cdot PO_3)^{2-}$ (35). Comparison of the -NH- group deprotonatation energy of $(2Mg^{2+}\cdot O_3P\text{-}NH\text{-}PO_3)^0$ with that for $H_4\cdot O_3P\text{-}NH\text{-}PO_3$ shows that the dimagnesium complex is less acidic than the fully protonated form which also has a net neutral charge. Direct release of H^+ from $(Mg^{2+}\cdot O_3P\text{-}NH\text{-}PO_3)^{2-}$ or $(2Mg^{2+}\cdot O_3P\text{-}NH\text{-}PO_3)^0$ is not thermodynamically feasible. These in vacuo calculations on small models likely have compensating limitations in the estimation of the ability of Mg^{2+} to facilitate deprotonation because additional ligands to a Mg^{2+} makes each ligand less acidic (44, 45), while the lack of a polar solvation environment in the models may lead to underestimation of the acidity.

DISCUSSION

The AdoMet dependences of the high affinity, slow-binding inhibition by the intermediate analogue PNPNP and the product analogue PNP provide new insights into the active site of AdoMet synthetase. The UV spectroscopic results reveal that the protein conformation is perturbed upon formation of the $E\cdot 2Mg^{2+}\cdot AdoMet\cdot PNPNP$ complex to a greater extent than in the $E\cdot 2Mg^{2+}\cdot PNPNP$ complex. This spectral difference is also seen with PPPi and is reminiscent of the ~30-fold enhancement of the k_{cat} for PPPi hydrolysis by AdoMet and the transition state analogue behavior of PNPNP. The slow rates of UV absorption changes for PNPNP binding in the presence of AdoMet demonstrate that two unimolecular events follow the initial binding step (Scheme 1B). The spectral features in the 280−310 nm region indicate the perturbation of both tryptophan and tyrosine residues, while the feature seen near 256 nm that is observed solely in the presence of AdoMet probably arises from perturbations of the adenine chromaphore. The crystal structure of the enzyme·$2Mg^{2+}\cdot ADP\cdot Pi$ complex shows that the only aromatic residue in the active site is phenylalanine-230, and the nearest tryptophan is a surface residue some 15 Å distant (46). Thus, the spectra suggest long-range conformational alterations upon complex formation, consistent with observations of altered tryptophan fluorescence upon ligand binding (33). Circular dichroism spectra were previously found to be indistinguishable for the free enzyme and the enzyme·$2Mg^{2+}\cdot AdoMet\cdot PNPNP$ complex, indicating

Table 3: Equilibrium and Rate Constants for Isomerizations of AdoMet Synthetase Complexes[a]

complex	K_{eq}	$k_{forward}$ (s^{-1})	$k_{reverse}$ (s^{-1})	ref
$E\cdot 2Mg^{2+}\cdot AdoMet\cdot PNPNP$	0.027	1.7	63	this work
$\{E\cdot 2Mg^{2+}\cdot AdoMet\cdot PNPNP\}'$	700	0.14	0.0002	this work
free enzyme	1.5	>10	>10	*49*
$E\cdot 2Mg^{2+}\cdot ATP\cdot Met$	1.5	22	14	*48*
$E\cdot 2Mg^{2+}\cdot AdoMet\cdot PPPi$	8	33	4	*33*
$E\cdot 2Mg^{2+}\cdot AdoMet\cdot PPi\cdot Pi$	300	12	0.04	*33*

[a] In each case, the complex shown is the starting complex for the isomerization, e.g., the first isomerization is $E\cdot 2Mg^{2+}\cdot AdoMet\cdot PNPNP \rightarrow \{E\cdot 2Mg^{2+}\cdot AdoMet\cdot PNPNP\}'$.

that gross secondary structural changes do not occur upon binding (20). This is consistent with crystallographic comparisons of the structures of the free enzyme and several complexes which indicate overall rigidity of the tetrameric organization and the 383 residue protein backbone (22, 46, 47). Our recent work has demonstrated the presence of kinetically significant conformational changes during the catalytic cycle; however, these changes appear to be localized in a flexible 15-residue active site lid that does not contain aromatic residues (33, 48, 49). The rates of the lid isomerizations are 10−100 s^{-1}, faster than the rates seen with the interconversion of PNPNP complexes (Table 3).

The combined kinetic data for formation of the highest affinity complex, ($\{$enzyme·$2Mg^{2+}\cdot AdoMet\cdot PNPNP\}'$ in Scheme 1B) allow clarification of individual rates and equilibrium constants. The previously measured equilibrium constant for formation of the initial enzyme·$2Mg^{2+}\cdot AdoMet\cdot PNPNP$ complex of 38 nM and the measured second-order rate constant for PNPNP binding to form this complex (7 × 10^4 M^{-1} s^{-1}) allow calculation of the dissociation rate constant of 2.6 × 10^{-3} s^{-1}. Assuming that reversal of the second isomerization step is rate limiting in PNPNP dissociation at 2 × 10^{-4} s^{-1}, the equilibrium constant for this step is (0.14 s^{-1}/2 × 10^{-4} s^{-1}) = 700. The net equilibrium constant for the isomerizations of 19 thus yields an equilibrium constant for the first isomerization of 0.027, which in combination with the forward rate observed in the stopped-flow (1.7 s^{-1}) provides a reverse rate constant for the first isomerization step of 63 s^{-1}. The rates for the first isomerization resemble those previously reported for the free enzyme, the complexes $E\cdot 2Mg^{2+}\cdot ATP\cdot Met$, $E\cdot 2Mg^{2+}\cdot AdoMet\cdot PPPi$ and $E\cdot 2Mg^{2+}\cdot AdoMet\cdot PPi\cdot Pi$, while the second isomerization is substantially slower (Table 3).

The ^{31}P NMR spectra demonstrate that the electronic environment of each phosphorus nucleus is distinct in the enzyme-bound complexes. The loss of symmetry of PNPNP upon binding to the enzyme is a phenomenon similar to that seen for (P_1, P_5)-diadenosine pentaphosphate (Ap5A) bound to adenylate kinase (50), and presumably reflects the electronic differences at the sites for AdoMet formation and of phosphoryl transfer. The comparison of ^{31}P chemical shifts for complexes of the form $E\cdot 2Mg^{2+}\cdot AdoMet\cdot$(PNP or PPNP or PNPNP) suggests assignments of the resonances to specific nuclei (Figure 6). A resonance near −3 ppm that is observed in complexes with both PNPNP and PPNP is likely to arise from the phosphorus with the common N−PO_3 bonding, that which occupies the γ phosphoryl group binding site. The peak with a chemical shift near −2 ppm observed

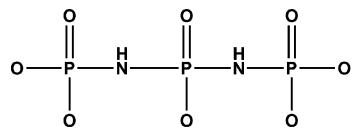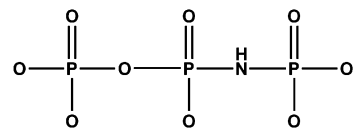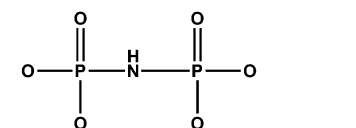| δ (ppm)			Δδ (ppm)		
α	β	γ	α	β	γ
-1.9 (+1.2)	+0.5 (+2.6)	-2.9 (1.2)	-3.1	-2.1	-4.1
-11 (-8.7;-5.2*)	-8.2 (-4.5)	-3.3 (+0.2)	-2.3 (-5.8*)	-3.7	-3.5
-2.2(+3.3)	+4.1 (+3.3)		-5.5	+0.8	

FIGURE 6: Proposed ^{31}P chemical shifts for AdoMet synthetase complexes. The left column lists observed shifts in protein complexes, and the chemical shifts in the absence of protein are in parentheses. The right column lists the changes in shifts between free and bound species. The first entry for free compounds associated with O_3P-O-PO$_2$-NH-PO$_3$ reflects Mg^{2+}·AMPPNP, while second entry for the O_3P-O group (denoted by an asterisk) is the shift of Mg^{2+}·PPPi, which is a more appropriate model for this moiety.

with both PNP and PNPNP complexes presumably arises from the O_3P-N- group at the α phosphoryl group site; in PPNP the bonding of the cognate atom is O_3P-O- and the corresponding resonance is at −11 ppm which is better compared to the chemical shift of a terminal group of Mg^{2+}· PPPi (−5.2 ppm) than to the shift of the differently bonded α phosphoryl group of Mg^{2+}·AMPPNP (+0.2 ppm). Thus, by elimination, the resonance of the phosphorus at the β phosphoryl group site, for which bonding varies from N-PO$_2$-O in PPNP to N-PO$_2$-N in PNPNP and a terminal N-PO$_3$ in PNP, falls at −8.2, +0.5, and +4.1 ppm, respectively. Comparison of shifts for PNP, PPNP, and PNPNP indicates that at both the α and β sites the replacement of an O by an N atom leads to a ∼+7 to +10 ppm chemical shift in the bound species, smaller than the range of +9 to +13 ppm in solution (34).

Using the proposed assignments for bound PNPNP resonances of the α, β, and γ phosphorus atoms at −1.9, +0.5, and −2.9 ppm, the shifts upon PNPNP binding in the presence of AdoMet are for end phosphorus atoms from +1.2 to −1.9 and −2.9 ppm (net −3.1 and −4.1 ppm), and for the middle phosphorus from +2.6 to +0.5 ppm, a change of −2.1 ppm (see Figure 6). Not surprisingly, the electronic environments of the terminal phosphorus atoms are both perturbed in the enzyme·$2Mg^{2+}$·PNPNP·AdoMet complex compared to the solution environment. The assignments imply that in the complex lacking AdoMet the chemical shift of the γ phosphorus is nearly unchanged at −3 ppm, while the other two ^{31}P nuclei have 1−3 ppm more positive shifts. Because we could not obtain bound spectra for PNP or PPNP

complexes in the absence of AdoMet, it is not sensible to propose assignments for the PNPNP resonances in the enzyme·$2Mg^{2+}$·PNPNP complex. The complex relationship between molecular structure and ^{31}P chemical shifts thwarts deduction of the ionization state of bound PNPNP from these data (51). Nevertheless, the chemical shifts upon PNPNP binding to the enzyme, and the changes in shifts when AdoMet is also present, clearly reflect unusual alterations in the electronic environment of the phosphorus atoms, effects that are not mimicked by simple solution ionizations. Furthermore, the sensitivity of two of the chemical shifts to the presence of AdoMet correlates with the variation in PNPNP affinity. Literature values for changes in ^{31}P chemical shifts upon ligand binding to proteins indicate that shifts are typically less than ± 3.5 ppm in the absence of changes in covalent bonding; alterations tend to occur at single phosphoryl groups in polyphosphate compounds rather that throughout the polyphosphate chain (37, 38, 52). Thus, the changes in chemical shifts of the phosphorus atoms upon PNPNP binding to AdoMet synthetase are near the extreme of the reported values, and are distributed throughout the structure, suggesting that they reflect a distinctly perturbed structure.

The inability to obtain ^{15}N NMR data for enzyme-bound PNPNP complexes prevented conclusive determination of whether the imido nitrogen(s) are protonated at the active site and whether the protonation state changes when AdoMet binds. The failure to observe signals may arise from unexpectedly broad lines due to chemical exchange such as -NH- → -N[−]- interconversion or to very long T_1 relaxation times.

The EPR spectra of Mn^{2+} complexes show that two Mn^{2+} ions bind cooperatively to the active site. The large number of spectral lines shows that the exchange coupling constant is comparable to the [55]Mn hyperfine coupling constant of 90 G and is similar in the presence and absence of AdoMet. In the limits of strong coupling, the spectra would appear as a set of 11 lines at 45 G intervals, while spectra of uncoupled ions are based on 90 G intervals. The similar coupling strengths demonstrate that the intermetal distance is not very different in the enzyme·$2Mn^{2+}$·PNPNP and enzyme·$2Mn^{2+}$· PNPNP·AdoMet complexes because for a common bonding pathway the magnitude of exchange coupling is exponentially dependent on distance between the paramagnetic centers (43). Thus, the EPR data suggest that changes in metal ion coordination are not involved in the AdoMet enhancement of PNPNP affinity.

The computational results for the PNP model complexes indicate that the P−N bond distance would decrease upon ionization of the nitrogen, from 1.857 to 1.692 Å in the monomagnesium complex and from 1.878 to 1.730 Å in the dimagnesium complex. The decrease in bond distance implies an increase in bonding electron density, which could cause a substantial change in chemical shifts. The calculation of changes in phosphorus isotropic chemical shifts of the relatively small magnitude observed herein is not yet well established; thus, computational models cannot be relied upon (cf. ref 32).

In all, the results favor a model in which slow deprotonation of the -NH- group in the P$_α$-NH-P$_β$ moiety results in the complex binding process (Scheme 1B). Proton abstraction would be thermodynamically more facile for the less charged
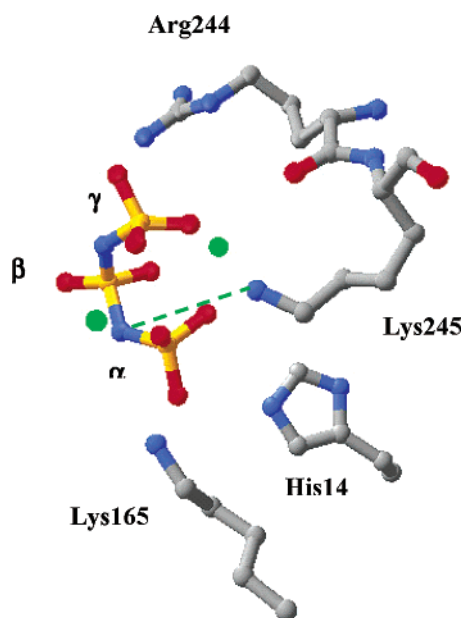
FIGURE 7: Model for PNPNP bound at the active site of AdoMet synthetase. The Mg^{2+} ion at right is coordinated to all three phosphoryl groups, and the second is coordinated to the two terminal groups. Polar residues near PNPNP are shown. The proposed interaction of the ϵ amino group of lysine-245 with the -NH- group occupying the position for the $\alpha-\beta$ bridge oxygen of ATP is illustrated. Unaltered protein coordinates were taken from the PDB file 1mxa (*46*), and the model for PNPNP was superimposed. Atoms are colored by the CPK scheme with Mg^{2+} in green.

PNP than PNPNP, consistent with the more rapid isomerization kinetics of PNP complexes.

In view of the proposal that deprotonation of a P-NH-P group is the cause of the uniquely high affinity of PNP and PNPNP, crystal structures of the enzyme were examined with a model for bound PNPNP replacing PPi and Pi in the structure (Figure 7). Crystallographic studies indicate that both metal ions are bound to all three phosphoryl groups in complexes with PPi plus Pi, or ADP plus Pi (*46*); however, tridentate coordination of both metal ions to an intact triphosphate chain appears to be geometrically improbable. More recent results for the E·2Mg^{2+}·AMPPNP·methionine complex show that one metal ion is coordinated to all three phosphoryl groups and the other metal ion is ligated to the α and γ phosphoryl groups of the nucleotide (PDB file 1P7L (*53*)). The group that might accept a proton is not unambiguous based on the structures, but candidates are residues lysine-165 and lysine-245 which have ϵ-amino nitrogens within 5 Å of the nitrogen of the P-NH-P model chain. Lysine-245 may have a suppressed pK due to its proximity of its amino group to the guanidinium of arginine-244 (ca. 6 Å), and thus could be a proton acceptor. Arginine-244 has been implicated as a key residue in the tight binding of PNPNP because in the Arg244Leu mutant protein the affinity of PNPNP is reduced 5000-fold and the slow binding steps are eliminated (*20*). Unfortunately, mutant proteins that are altered at lysine-245 are not correctly folded (*54*), precluding reliable deductions from their properties (*54*). Mutants at lysine-165 have essentially unaltered catalytic properties, suggesting that this residue is unlikely to be involved (*54*). Alternatively, a water (or hydroxide) that is coordinated to Mg^{2+} would necessarily be in proximity to the -NH- groups and could be a proton acceptor. The caveat remains that the

side chain conformational changes which clearly accompany formation of the maximally inhibitory complexes render tenuous any interpretations based on the available crystallographic data from complexes with other ligands.

AMPPNP and PNP have widely been considered to be inert to enzyme catalyzed reactions and as representative stable analogues of ATP and PPi (*24, 55–57*). Nevertheless, there are other examples of unforeseen interactions and reactions in protein complexes. AMPPNP is a slow binding inhibitor of the F1-ATPase, suggesting a different interaction than that with ATP (*58*). Contrariwise, there are examples of enzymes that hydrolyze these compounds. AMPPNP is a substrate for the sodium-potassium ATPase (*59*), and PNP is a substrate for apyrase (*60*). Crystallographic studies of the neutral $[Co^{3+}(NH_3)_4(HO_3P-NH-PO_3)]$ complex showed that protonation occurs on a phosphate oxygens rather than the nitrogen (*60*). Nevertheless, the apyrase-catalyzed hydrolysis of both $O_3P-NH-PO_3$ and $Co^{3+}(NH_3)_4(O_3P-NH-PO_3)$ suggested that protonation of the bridging imido nitrogen to a -NH_2^+- group occurred at the active site (*60*). In combination with our results that suggest deprotonation of the -NH- group at the AdoMet synthetase active site, it is clear that occasionally the imido analogues have unanticipated and uniquely informative interactions with proteins.

REFERENCES

1. Cantoni, G. L. (1975) *Annu. Rev. Biochem. 44*, 435–51.
2. Tabor, C. W., and Tabor, H. (1984) *Adv. Enzymol. Relat. Areas Mol. Biol. 56*, 251–82.
3. Markham, G. D. (2002) *Nature Encyclopedia of Life Sciences*, Nature Publishing Group, Macmillan Publishers Ltd., London, http://www.els.net/ [DOI: 10.1038/npg.els.0000662].
4. Coulter, A. W., Lombardini, J. B., Sufrin, J. R., and Talalay, P. (1974) *Mol. Pharmacol. 10*, 319–34.
5. Goldberg, B., Rattendi, D., Lloyd, D., Sufrin, J. R., and Bacchi, C. J. (1998) *Biochem. Pharmacol. 56*, 95–103.
6. Sufrin, J. R., Lombardini, J. B., and Keith, D. D. (1982) *Biochem. Biophys. Res. Commun. 106*, 251–5.
7. Sufrin, J. R., Lombardini, J. B., and Alks, V. (1993) *Biochim. Biophys. Acta 1202*, 87–91.
8. Lavrador, K., Allart, B., Guillerm, D., and Guillerm, G. (1998) *J. Enzyme Inhib. 13*, 361–7.
9. Lavrador, K., Guillerm, D., and Guillerm, G. (1998) *Bioorg. Med. Chem. Lett. 8*, 1629–34.
10. Vrudhula, V. M., Kappler, F., and Hampton, A. (1987) *J. Med. Chem. 30*, 888–94.
11. Lim, H., Kappler, F., Hai, T. T., and Hampton, A. (1986) *J. Med. Chem. 29*, 1743–8.
12. Kramer, D. L., Sufrin, J. R., and Porter, C. W. (1987) *Biochem. J. 247*, 259–65.
13. Kramer, D. L., Sufrin, J. R., and Porter, C. W. (1988) *Biochem. J. 249*, 581–6.
14. Porter, C. W., Sufrin, J. R., and Keith, D. D. (1984) *Biochem. Biophys. Res. Commun. 122*, 350–7.
15. Kappler, F., Hai, T. T., Cotter, R. J., Hyver, K. J., and Hampton, A. (1986) *J. Med. Chem. 29*, 1030–8.
16. Kappler, F., Hai, T. T., and Hampton, A. (1986) *J. Med. Chem. 29*, 318–22.
17. Kappler, F., and Hampton, A. (1990) *J. Med. Chem. 33*, 2545–51.
18. Kappler, F., Vrudhula, V. M., and Hampton, A. (1987) *J. Med. Chem. 30*, 1599–603.
19. Kappler, F., Vrudhula, V. M., and Hampton, A. (1988) *J. Med. Chem. 31*, 384–9.
20. Reczkowski, R. S., and Markham, G. D. (1999) *Biochemistry 38*, 9063–8.
21. Reczkowski, R. S., Taylor, J. C., and Markham, G. D. (1998) *Biochemistry 37*, 13499–506.
22. Fu, Z., Hu, Y., Markham, G. D., and Takusagawa, F. (1996) *J. Biomol. Struct. Dyn. 13*, 727–39.

23. Markham, G. D., Hafner, E. W., Tabor, C. W., and Tabor, H. (1980) *J. Biol. Chem. 255*, 9082−92.
24. Ma, Q. F., Kenyon, G. L., and Markham, G. D. (1990) *Biochemistry 29*, 1412−6.
25. Xiang, B., and Markham, G. D. (1997) *Arch. Biochem. Biophys. 348*, 378−82.
26. Marat, K. (2000) Spinworks v. 1.2, University of Manitoba, ftp://davinci.chem.umanitoba.ca/pub/marat/SpinWorks.
27. Becke, A. D. (1993) *J. Chem. Phys. 98*, 5648−52.
28. Lee, C. T., Yang, W. T., and Parr, R. G. (1988) *Phys. Rev. B 37*, 785−9.
29. Frisch, M. J., Trucks, G. W., Schlegel, H. B., Scuseria, G. E., Robb, M. A., Cheeseman, J. R., Zakrzewski, V. G., Montgomery, J. A., Jr., Stratmann, R. E., Burant, J. C., Dapprich, S., Millam, J. M., Daniels, A. D., Kudin, K. N., Strain, M. C., Farkas, O., Tomasi, J., Barone, V., Cossi, M., Cammi, R., Mennucci, B., Pomelli, C., Adamo, C., Clifford, S., Ochterski, J., Petersson, G. A., Ayala, P. Y., Cui, Q., Morokuma, K., Malick, D. K., Rabuck, A. D., Raghavachari, K., Foresman, J. B., Cioslowski, J., Ortiz, J. V., Stefanov, B. B., Liu, G., Liashenko, A., Piskorz, P., Komaromi, I., Gomperts, R., Martin, R. L., Fox, D. J., Keith, T., Al-Laham, M. A., Peng, C. Y., Nanayakkara, A., Gonzalez, C., Challacombe, M., Gill, P. M. W., Johnson, B., Chen, W., Wong, M. W., Andres, J. L., Gonzalez, C., Head-Gordon, M., Replogle, E. S., and Pople, J. A. (1998) Gaussian, Inc., Pittsburgh, PA.
30. Wolinski, K., Hilton, J. F., and Pulay, P. (1990) *J. Am. Chem. Soc. 112*, 8251−60.
31. Brender, J. R., Taylor, D. M., and Ramamoorthy, A. (2001) *J. Am. Chem. Soc. 123*, 914−22.
32. Potrzebowski, M. J., Assfeld, X., Ganicz, K., Olejniczak, S., Cartier, A., Gardiennet, C., and Tekely, P. (2003) *J. Am. Chem. Soc. 125*, 4223−32.
33. McQueney, M. S., Anderson, K. S., and Markham, G. D. (2000) *Biochemistry 39*, 4443−54.
34. Tran-Dinh, S., and Roux, M. (1977) *Eur. J. Biochem. 76*, 245−9.
35. Reynolds, M. A., Gerlt, J. A., Demou, P. C., Oppenheimer, N. J., and Kenyon, G. L. (1983) *J. Am. Chem. Soc. 105*, 6475−6481.
36. Rosch, P. (1986) *Prog. Nucl. Magn. Reson. Spectrosc. 18*, 123−169.
37. Nageswara Rao, B. D. (1983) in *Biological Magnetic Resonance* (Reuben, J., Ed.) pp 75−128, Plenum Press, New York.
38. Gerothanassis, I. P., Barrie, P. J., Birdsall, B., and Feeney, J. (1994) *Eur. J. Biochem. 226*, 211−8.
39. Schalk-Hihi, C., and Markham, G. D. (1999) *Biochemistry 38*, 2542−50.
40. Jaffe, E. K., Markham, G. D., and Rajagopalan, J. S. (1990) *Biochemistry 29*, 8345−50.
41. Smith, G. M., Yu, L. P., and Domingues, D. J. (1987) *Biochemistry 26*, 2202−7.
42. Markham, G. D. (1981) *J. Biol. Chem. 256*, 1903−9.
43. Reed, G. H., and Markham, G. D. (1984) in *Biological Magnetic Resonance* (Reuben, J., Ed.) pp 73−142, Plenum Press, New York.
44. Katz, A. K., Glusker, J. P., Markham, G. D., and Bock, C. W. (1998) *J. Phys. Chem. B 102*, 6342−50.
45. Markham, G. D., Glusker, J. P., Bock, C. L., Trachtman, M., and Bock, C. W. (1996) *J. Phys. Chem. 100*, 3488−97.
46. Takusagawa, F., Kamitori, S., and Markham, G. D. (1996) *Biochemistry 35*, 2586−96.
47. Takusagawa, F., Kamitori, S., Misaki, S., and Markham, G. D. (1996) *J. Biol. Chem. 271*, 136−47.
48. Taylor, J. C., Takusagawa, F., and Markham, G. D. (2002) *Biochemistry 41*, 9358−69.
49. Taylor, J. C., and Markham, G. D. (2003) *Arch. Biochem. Biophys. 415*, 164−71.
50. Nageswara Rao, B. D., and Cohn, M. (1977) *Proc. Natl. Acad. Sci. U.S.A. 74*, 5355−7.
51. Un, S., and Klein, M. P. (1989) *J. Am. Chem. Soc. 111*, 5119−24.
52. Ray, B. D., Moore, J. M., and Rao, B. D. (1990) *J. Inorg. Biochem. 40*, 47−57.
53. Komoto, J., Yamada, T., Takata, Y., Markham, G. D., and Takusagawa, F. (2004) *Biochemistry 43*, 1821−1831.
54. Taylor, J. C., and Markham, G. D. (2000) *J. Biol. Chem. 275*, 4060−5.
55. Yount, R. G., Babcock, D., Ballantyne, W., and Ojala, D. (1971) *Biochemistry 10*, 2484−9.
56. Yount, R. G. (1975) *Adv. Enzymol. Relat. Areas Mol. Biol. 43*, 1−56.
57. Lin, I., Knight, W. B., Hsueh, A., and Dunaway-Mariano, D. (1986) *Biochemistry 25*, 4688−92.
58. Philo, R. D., and Selwyn, M. J. (1974) *Biochem. J. 143*, 745−9.
59. Schuurmans Stekhoven, F. M., Swarts, H. G., De Pont, J. J., and Bonting, S. L. (1983) *Biochim. Biophys. Acta 736*, 73−8.
60. Haromy, T. P., Knight, W. B., Dunaway-Mariano, D., and Sundaralingam, M. (1983) *Biochemistry 22*, 5015−21.

BI035953Z